Journal of MATERIALS RESEARCH

Invited Paper
DOI: 10.1557/jmr.2018.463

Glucomannan asymmetric membranes for wound dressing

Giovana Maria Genevro[1,b], Reginaldo Jose Gomes Neto[1,b], Letícia de Almeida Paulo[2], Patrícia Santos Lopes[2], Mariana Agostini de Moraes[3], Marisa Masumi Beppu[1,a)]

[1]School of Chemical Engineering, Department of Materials and Bioprocess Engineering, University of Campinas, Campinas, SP 13083-852, Brazil
[2]Environmental, Chemical and Pharmaceutical Sciences Institute, Department of Pharmaceutical Sciences, Universidade Federal de São Paulo, Diadema, SP 09913-030, Brazil
[3]Environmental, Chemical and Pharmaceutical Sciences Institute, Department of Chemical Engineering, Universidade Federal de São Paulo, Diadema, SP 09913-030, Brazil
[a)]Address all correspondence to this author. e-mail: beppu@feq.unicamp.br
[b)]These authors contributed equally to this work.

Received: 24 June 2018; accepted: 20 November 2018

Asymmetric membranes present promising characteristics for wound dressing applications. A porous structure uptakes the wound exudate, whereas an occlusive layer (upper film) inhibits the microbial penetration and prevents an excessive loss of water. Konjac glucomannan (KGM) is a natural polysaccharide that has been investigated as wound dressings in the form of films, sponges, and hydrogels due to its flexibility, swelling capacity, biocompatibility, and low cost. However, there are no studies on literature regarding the development of KGM asymmetric membranes. In this study, we investigated a new casting–freezing process for the production of KGM asymmetric membranes. The scanning electron microscopy and thermogravimetric analyses indicated an asymmetric morphology and a good thermal stability of the membrane samples, respectively. Moreover, biological, mechanical, and fluid-handling capacity tests showed that the membrane is biocompatible and resistant to handling structure, which was also able to retain the ideal moist conditions for wound healing.

Introduction

The skin is the largest organ in the human body and acts as a primary barrier against infectious agents. Also, it is responsible for regulating the body temperature, preventing the loss of body fluids, and storing a large number of nerve endings [1]. More than 20 million patients suffer from chronic skin injuries worldwide and the healing process for those injuries are usually slow, expansive, and poorly effective [2, 3]. In this context, many efforts have been made to aim the development of new wound dressings that could promote a rapid healing and minimize the patient pain [4].

An ideal wound dressing should be able to absorb the wound exudates, protect the wound injuries from secondary infections, provide adequate gaseous exchanges, and regulate the release of growth factors and cytokines. Furthermore, it should be elastic, biocompatible, resistant to handling, nontoxic, and nonantigenic [5]. Among the desired characteristics of a high-performance wound dressing, the maintenance of an optimal moisture environment plays a key role in the wound healing process [6]. A suitable moisture content prevents the dehydration of the tissue and favors the autolytic debridement. Moreover, the moisture protects the nerve endings from dryness and exposure, which is directly related to pain. Also, moisture keeps cells viable, stimulating them to release growth factors and proliferate [1, 3].

Different material structures have been investigated aiming the development of new dressings that are able to retain the ideal moisture environment for healing, protect the wound injury against microorganism, and resist to the natural skin deformations. The occlusive dressings are resistant to handling and impermeable, but they are not capable of absorbing high levels of wound exudate [6]. On the other hand, microporous dressings present excellent capacity to uptake the body fluids, but they are ineffective in either controlling microbial penetration or preventing wound dehydration [1, 6].

This article has been corrected since its original publication. See doi:10.1557/jmr.2019.315.

https://doi.org/10.1557/jmr.2018.463 Published online by Cambridge University Press

© Materials Research Society 2019. This is a work of the U.S. Government and is not subject to copyright protection in the United States.

One unique strategy for designing high-performance wound dressings is by combining an occlusive surface with a porous structure in the so-called asymmetric membranes. These membranes present a stratified morphology similar to the healthy skin anatomy and are able to create a suitable environment for a better wound healing process [1]. For instance, asymmetric membranes of chitosan and polyurethane presented high capacity to drain the exudate and at the same time prevent the invasion of microorganisms, thereby surpassing the limitations presented by the commercial wound dressings [7, 8, 9, 10, 11, 12, 13].

Most of the asymmetric membranes are prepared by dry-/wet-phase inversion techniques, which require both volatile solvent and coagulant bath for promoting the polymer precipitation [1]. In these processes, a top dense layer is formed by evaporating the casting solution prior to its immersion in the coagulating bath, whereas a porous layer is formed during the phase inversion that takes place at the interface of the casting solution. However, most of the solvents and non-solvents used in the phase inversion processes are cytotoxic, requiring an additional step for purification. Moreover, these processes are limited to a small number of either synthetic or natural polymers [1].

Konjac glucomannan (KGM) is a natural polymer belonging to the mannan family and is extracted from tubers of the *Amorphophallus konjac* plant. It is a neutral polysaccharide composed of D-mannose and D-glucose monomers bound by β-linkage (1–4). KGM-based materials present promising properties for wound dressing applications due to its elasticity, swelling capacity, and low cost [14, 15, 16]. Furthermore, alkali-treated KGM materials are biocompatible with fibroblast and keratinocyte cells, accelerating the wound contraction and reepithelialization process [17]. KGM is also a versatile polymer, which can be either cast in the form of occlusive films [17, 18] or freeze-dried in the form of sponges, hydrogels, and aerogels [19, 20, 21]. However, there are no studies on literature regarding the development of KGM asymmetric membranes.

In this study, we investigated a new process for the production of KGM asymmetric membranes. We explored the casting followed by a freezing process to create a combination of occlusive and porous structures. Scanning electron microscopy (SEM) and thermal analyses were performed to evaluate the morphology and thermal stability of the membranes. Moreover, mechanical and fluid-handling tests were performed, as well as antimicrobial and cytotoxicity assays, to evaluate the membrane performance as a wound dressing. The results of this work show a simple and inexpensive process for the production of an asymmetric membrane of KGM. These membranes presented a good biocompatibility to mammalian cells, resistance to handling, and the capacity to both inhibit the microbial penetration and retain the ideal moist conditions for the wound healing.

Results and discussion

Structure and morphology

Figure 1(a) shows the photograph of the KGM asymmetric membrane. The samples presented a resistant and flat film on the top and a soft and spongy structure on the bottom. These macroscopic observations are in agreement with the SEM micrographs shown in Figs. 1(b)–1(d). A smooth and flat surface was observed on the top layer [Fig. 1(c)], whereas a porous structure with a mean pore size of 145 ± 15 μm and

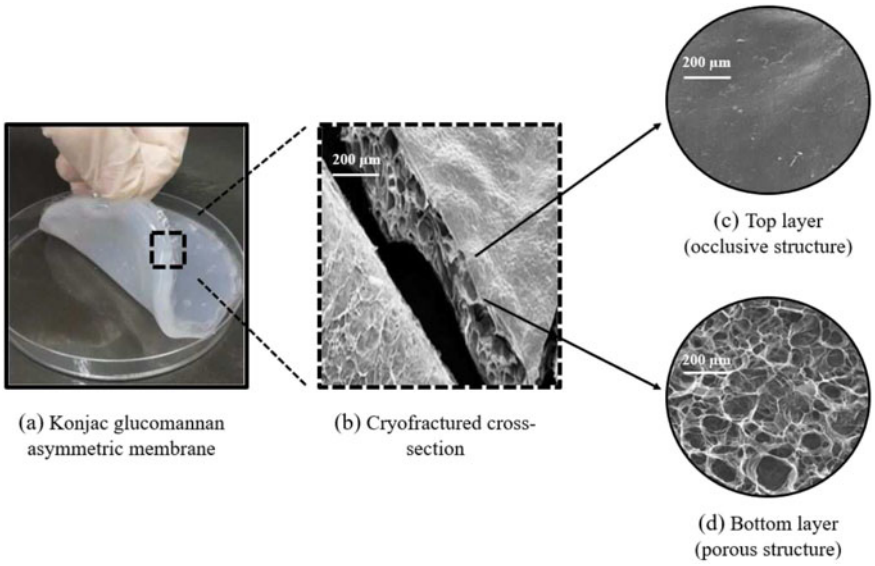


Figure 1: (a) Photograph of the KGM asymmetric membranes. (b) SEM micrograph of the cryofractured cross-section of the KGM membrane. Occlusive and porous layers faced up at the right and left side of the picture, respectively. (c) SEM micrograph of the occlusive surface (upper layer) of the KGM asymmetric membrane. (d) SEM micrographs of the porous surface of the KGM asymmetric membrane.

https://doi.org/10.1557/jmr.2018.463 Published online by Cambridge University Press

© Materials Research Society 2019. This is a work of the U.S. Government and is not subject to copyright protection in the United States.

a porosity of 58 ± 4% was observed on the bottom layer [Fig. 1(d)]. These values of mean pore size and membrane porosity agree with those found for other asymmetric membranes and scaffolds designed for tissue engineering [1, 29]. All membrane samples also retained their structural integrity at room temperature. Thus, the KGM asymmetric membrane can provide a trade-off between an occlusive layer, providing better mechanical properties, and a porous structure, providing a better environment for the skin regeneration.

The asymmetric structure shown in the SEM micrographs is a result of differences in the water availability between the bulk and the top layers of the KGM solution [30]. During the casting process, the top layers of the KGM solution present a water loss rate higher than that of the bottom layers due to the temperature gradient along the bulk of the solution. In addition, the jellification in alkaline solution creates both new hydrogen bonds and hydrophobic interactions among the KGM chains, thereby inhibiting the diffusion of water molecules between the layers of the solution [31, 32]. Since the KGM solution was partially dried, during the freezing step, ice crystals grow isotropically in the bulk of the water-rich bottom layers, leading to the formation of a porous structure. On the other hand, the freezing of the KGM-rich layers on the top of the solution produced an occlusive surface. If the KGM solution were air-dried to constant weight, it would result in the production of a completely occlusive membrane, as already shown in the literature [17].

Thermal studies

The thermal stability of the asymmetric membrane was investigated by TGA and its thermograms are shown in Fig. 2. The membrane weight loss from 25 to 150 °C was assigned to the loss of moisture, which represents 10% for the initial weight. The thermal degradation of KGM started at 240 °C and reached a maximum weight loss rate at 340 °C. This temperature range is related to the degradation of the saccharide rings and the disintegration of polymer chains. Beyond 370 °C, the weight loss rate significantly decreased, leaving around 16% of the initial weight. The TGA results are in agreement with those of previous studies of KGM powders [33], thus indicating that the process of production of the asymmetric membranes did not affect the thermostability of the pure polymer.

Mechanical properties

Wound dressings must be flexible and strong enough to withstand the natural deformations of the human skin [34, 35]. Usually, a healthy human skin presents a tensile strength between 2.5 and 35 MPa [36, 38], a Young's modulus ranging from 4.6 to 20 MPa, and an elasticity from 70 to 78% [38, 39]. Figure 3 shows the mechanical properties of the KGM asymmetric membranes.

The membrane samples presented a tensile strength of 0.51 ± 0.12 MPa and an elastic modulus of 0.54 ± 0.10 MPa, which are significantly lower than the values found for the human skin. However, they also presented a resistance to handling, retaining their shape integrity over the experiments. On the other hand, an elongation at break of 80.8 ± 23.2% was observed for the membrane samples, indicating that they could resist to natural deformations of the human skin. It is important to point out that mechanical tests were performed in wet KGM membrane samples (after the freeze–thawing process). Thus, the water acted as a natural plasticizer, increasing the membrane's flexibility and decreasing their tensile strength [40].

Barrier properties

A healthy human skin has a moisture transmission rate of 204 ± 12 g/m^2 24 h [41, 42]. However, skin injuries might decrease its ability to retain moisture. Therefore, wound dressings should inhibit the moisture loss by the injured skin and also prevent the accumulation of exudate in the injured area, which could lead to the maceration of the healthy tissue. The FHC test measures the capacity of a wound dressing to either absorb body fluids or retain the ideal moisture conditions for the wound healing. The results of FHC tests of KGM membrane

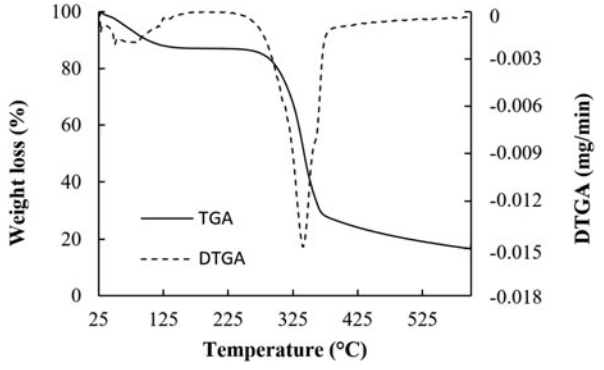


Figure 2: TGA and differential TGA (DGTA) thermograms of KGM asymmetric membranes.

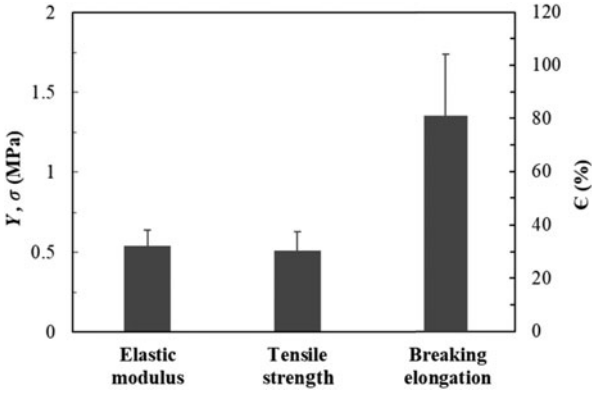


Figure 3: Mechanical properties of KGM asymmetric membranes.

https://doi.org/10.1557/jmr.2018.463 Published online by Cambridge University Press

© Materials Research Society 2019. This is a work of the U.S. Government and is not subject to copyright protection in the United States.

are shown in Fig. 4. Prior to the tests, the KGM membranes were already swollen in water due to the freeze–thaw process and were stored in wet conditions. Thereby, the negative values for the swelling capacity indicate that the water loss of the initial swollen sample was greater than the amount of water uptake over the test.

Commercially available wound dressings that also have an asymmetric structure present MVTR values ranging from 1670 to 12,350 g/m^2 24 h [24]. Thus, the MVTR of 3984.8 ± 1641.7 g/m^2 24 h observed for our KGM membranes agrees with the values found for solid brands, such as Active heal (Advanced Medical Solutions, Winsford, United Kingdom) and Allevyn adhesive (Smith & Nephew, London, United Kingdom). Moreover, it is known that wound injuries with granulation tissue or third-degree burns usually generate 3400–5100 g of exudates per day [1, 43]. Thus, the FHC values found for KGM membranes (3530.8 ± 1663.3 g/m^2 24 h) suggest that they could be used in the treatment of moderate and severe wound injuries with high levels of exudate production.

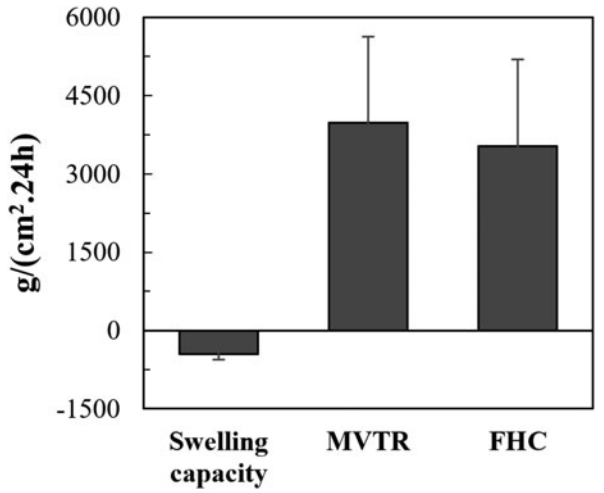


Figure 4: FHC of KGM asymmetric membranes.

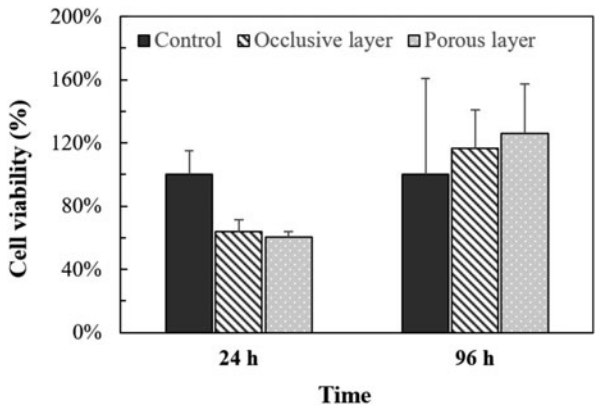


Figure 5: Cell viability of fibroblasts cells on the KGM asymmetric membranes.

Cytotoxicity studies

The results from the direct cytotoxicity studies are shown in Fig. 5. Within the first 24 h, the fibroblast cells presented a significantly lower metabolic activity when in contact with both sides of the KGM membrane than when in contact with the control. This result can be attributed to an extended lag phase of fibroblast growth cycle when they were exposed to an environment containing the KGM membrane. However, after 96 h, there is no statistical difference in the cell viability of all samples, thus indicating that both sides of the KGM membrane are biocompatible with the L929 fibroblasts.

The indirect cytotoxic assay was performed to investigate any leachable material that could adversely affect the cell metabolism. According to the ISO 10993-5, if the cell viability of the highest concentration of the sample extract is higher than 70% the material could be considered noncytotoxic. Nevertheless, the device cannot be determined to be unsuitable for a given clinical application based solely on cytotoxic data. The results of CHO cells viability on KGM membranes are shown in Fig. 6. The cell viability was higher than 80% for the extract concentrations ranging from 0.78 to 3.12%. However, for higher concentrations of sample extract, the cell viability decreased to around 65%. Previous studies have indicated a good biocompatibility of KGM films and sponges with mammalian cells [17, 44]. Thus, the RPMI medium might be extracting any leachable material from the KGM membranes that did not favor the cell culture for a high extract concentration. For instance, ethanol and NaOH residue produced from sterilization and jellification steps, respectively, might be adversely affecting the CHO cells viability. Finally, it was observed that none of the sample membranes caused a reduction in cell viability to values below the IC50, which represents the death of 50% of the cells.

Antimicrobial activity

Figure 7 shows the antimicrobial activity of both sides of the KGM membranes against gram-negative (*P. aeruginosa* and *E. coli*) and gram-positive (*S. aureus*) bacterial strains and yeast (*C. albicans*) strains. No antimicrobial activity was observed for

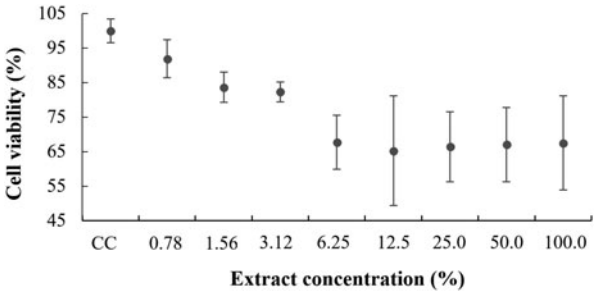


Figure 6: Cell viability of CHO cells on the KGM asymmetric membranes.

https://doi.org/10.1557/jmr.2018.463 Published online by Cambridge University Press

© Materials Research Society 2019. This is a work of the U.S. Government and is not subject to copyright protection in the United States.

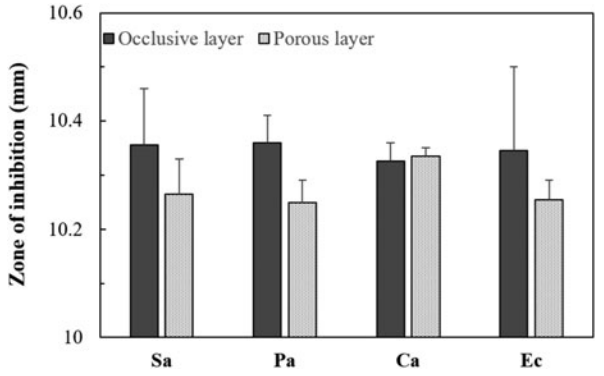


Figure 7: Antimicrobial activity of KGM membranes against *Staphylococcus aureus* (Sa), *Pseudomonas aeruginosa* (Pa), *Candida albicans* (Ca), and *Escherichia coli* (Ec).

the KGM asymmetric membranes since no halo of inhibition significantly greater than 10 mm was observed. These results were expected since there are no antimicrobial substances incorporated into the membranes that could leach out to the medium. However, both sides of the membrane presented a biostatic action, inhibiting the growth of all strains by contact. These results are in accordance with the results of previous studies on the antimicrobial activity of air-dried KGM membranes [18, 45].

Du et al. (2013) [18] have investigated the biostatic action of KGM–chitosan blend membranes and proposed that they might able to form a layer on the surface of the cell membrane, thus preventing the diffusion of nutrients into the cells. This proposition can be extended to the biostatic action also observed for the KGM asymmetric membranes, which might be able to create a physical barrier that blocks the entry of nutrients into gram-positive and gram-negative bacterial strains and yeast strains.

Antimicrobial penetration

The human skin provides a physical and chemical protection against microbial invasions. Layers of epithelial cells covered with keratin act as an effective physical barrier against microbial penetration. Furthermore, the periodic renewal of the skin cells inhibits microbial growth by removing any adhered microorganism [46]. Thus, wound dressings should perform similarly to a healthy human skin when it comes to antimicrobial control. For the microbial penetration tests, only the positive controls presented a cloudiness in the TBS medium. On the other hand, the KGM membranes and negative controls presented a clear and homogeneous medium. These results indicate that TSB was a suitable medium for microbial growth and that no microorganism was able to permeate through the KGM membranes.

Conclusion

The KGM membranes obtained by the novel casting–freezing process presented an asymmetric structure composed of a flat film on the top layer and a porous structure on the bottom layer. These membranes showed a good resistance to handling, a high percentage of elongation, and a suitable FHC when compared with other commercially available wound dressings. In addition, the biological tests indicated that the membranes are able to prevent microbial penetration and did not inhibit the skin cells viability. Therefore, the asymmetric membrane of KGM is a promising material for wound dressing applications due to its mechanical and barrier properties, biocompatibility, and low cytotoxicity.

Experimental

Preparation of the asymmetric membranes

KGM powder was supplied by Konjac Foods (Sunnyvale, California) with an average molecular weight of 1.48×10^6 Da and a polydispersity index of 1.01, which were measured by gel permeation chromatography. The KGM powder was stirred for 4 h with ultrapure water to prepare a 1% (w/v) solution. Then, sodium hydroxide was added to the solution (KGM gelling agent) until it reaches a final concentration of 0.1 mol/L. For the production of the asymmetric membranes, 60 g of KGM/NaOH solution was cast onto a polystyrene plate (d = 9 cm) and dried at 60 °C until it reaches 20% of the initial mass. Next, the samples were frozen at −6 °C for 24 h. Finally, the asymmetric membranes were thawed and rinsed with ultrapure water until the wash solution reaches a neutral pH.

Structure and morphology

The morphology of the membrane samples (1 cm^2) was observed by SEM (LEO 440i; LEO ElectronMicroscopy, Cambridge, United Kingdom). The cross-section micrographs were obtained from cryofractured membranes by immersing them into liquid nitrogen. The average pore size and membrane porosity were calculated by the NIH ImageJ (National Institutes of Health, Madison, Wisconsin) software (n = 7). Prior to SEM analysis, the membranes were freeze-dried in liquid nitrogen and coated with gold.

Thermal stability

Thermogravimetric analysis (TGA) and differential TGA of membrane samples (6 mg) were performed with TGA-50M SHIMADZU (Shimadzu Corp., Kyoto, Japan), with temperature ranging from 25 to 600 °C. The heating rate was 10 °C/min,

https://doi.org/10.1557/jmr.2018.463 Published online by Cambridge University Press

© Materials Research Society 2019. This is a work of the U.S. Government and is not subject to copyright protection in the United States.

and the nitrogen flow rate was 50 mL/min. All membrane samples were previously freeze-dried.

Mechanical properties

Mechanical tests were performed according to the ASTM D882-02 [22] with a TA.XT2 tensile tester (Stable Microsystems SMD, Godalming, United Kingdom) with a load cell of 50 N. The membrane samples were cut into strips of 7 × 2.5 cm (w) and gently pressed between filter papers to remove the excess of water. Then, all samples were incubated for 48 h in a desiccator with 50% of relative humidity. The thickness (e) of the membranes was measured by a digital micrometer (MDC-25S; Mitutoyo, Suzano, Brazil). The distance between the claws of the tensile tester was 5 cm (l) and the speed of the test was 10 mm/s. The tensile strength (σ_b) and breaking elongation (ϵ_b) of membrane samples were calculated as follows:

$$\sigma_b = F/(e \times w) \quad ,$$

$$\epsilon_b = (d/l) \times 100 \quad ,$$

where d is the final distance covered by the claws of the tensile tester.

Barrier properties

The fluid-handling capacity (FHC) of the membrane samples was investigated according to the BS EN 13726-1 method for hydrocolloids and dressings [23]. This test measures the capacity of a membrane to remove exudate by the sum of its swelling capacity and moisture vapor transmission rate (MVTR). For the FHC test, all samples were first sterilized with ethanol 70% (v/v) and then rinsed with phosphate-buffered saline (PBS). An aqueous solution of NaCl 142 mmol/L and $CaCl_2$ 1.25 mmol/L was used as a simulated exudate fluid (SEF) [24]. Then, the samples were weighed (m_1) and placed at the upper edges of modified Paddington cups [test area of 5.72 cm^2 (A)], which were previously filled with 20 mL of SEF. Next, the systems were weighed (m_2) and inverted, so that the membranes could be in direct contact with the SEF. The systems were incubated at 37 °C for 24 h (t) in a desiccator containing silica gel. After the incubation period, the systems were left at room temperature for 30 min and both membranes (m_3) and systems (m_4) were reweighed. The swelling capacity, MVTR, and FHC were calculated as follows:

$$\text{Swelling capacity}\left(\text{g/cm}^2 \cdot 24\ \text{h}\right) = (m_3 - m_1)/t \cdot A \quad ,$$

$$\text{MVTR}\left(\text{g/cm}^2 \cdot 24\ \text{h}\right) = (m_4 - m_2)/t \cdot A \quad ,$$

$$\text{FHC}\left(\text{g/cm}^2 \cdot 24\ \text{h}\right) = \text{Swelling capacity} + \text{MVTR} \quad .$$

Direct cytotoxicity

The direct cytotoxicity of KGM asymmetric membrane was tested on L929 fibroblast cells by the resazurin method. Viable cells when in direct contact with the resazurin indicator can reduce it into resorufin, which is fluorescent [25]. For this test, the membrane samples were first cut into discs of 1.2 cm of diameter and decontaminated with ethanol 70% (v/v) and PBS. Then, the samples were placed in a 24-well plate and Teflon® O-rings were used to ensure that the discs did not float in the culture medium. The culture medium used was α-MEM (minimum essential medium eagle alpha modification) containing 10% of fetal bovine serum, 1% of fungizone, and 1% of penicillin–streptomycin. Plates without KGM membranes were used as positive controls. Then, L929 fibroblasts were spread on the faces of both membranes and controls at the concentration of 2 × 10^4 cells per well. Cells were cultured at 37 °C in an atmosphere of 5% CO_2. On first and fourth days, the culture medium was replaced and 10% of resazurin agent was added into the wells, which were incubated for more 3.5 h. Then, 100 µL of the solution was transferred to 96-well plates and the fluorescence intensity (FI) was measured on a microplate reader (Synergy HTX; Biotek, Winnoski, Vermont) at 530 and 590 nm. The cell viability was calculated as follows:

$$\text{Cell viability}(\%) = \left(\text{FI}_{\text{Sample}}/\text{FI}_{\text{Control}}\right) \times 100\% \quad .$$

Indirect cytotoxicity

The indirect cytotoxicity of membrane samples was investigated on Chinese hamster ovary (CHO) cells according to the ISO 10993-5 (2009) [26]. CHO is an established cell line, traditionally used in either cytotoxic or genotoxic tests. First, CHO cells were incubated at 37 °C in an atmosphere of 95% of relative humidity and 5% CO_2 and until reaching approximately 80% of subconfluent cells on the culture plate. The cellular detachment process was carried out using trypsin/ethylenediamine tetraacetic acid (EDTA) solution [0.05% (w/v) trypsin and 0.02% (w/v) EDTA in phosphate buffer of pH 7.2]. Then, the cells were cultivated in a 75 cm^2 flask with 10 mL of RPMI-appropriate culture medium supplemented with 10% fetal bovine serum (Gibco FBS, ThermoFisher, Carlsbad, California) and incubated again at 37 °C in an atmosphere of 5% CO_2. Simultaneously, the membrane samples were decontaminated with 70% (v/v) ethanol for 2 h and then rinsed with sterile PBS. After the decontamination process, the membranes were placed in sterile tubes and the serum-free culture medium was added in the ratio of 1 mL per 6 cm^2 of the membrane. Gauze material was used as a negative control, while latex was used as a positive control. Then, the tubes were incubated at 37 °C for 72 h. Next, the extracts were filtered with membranes

https://doi.org/10.1557/jmr.2018.463 Published online by Cambridge University Press

© Materials Research Society 2019. This is a work of the U.S. Government and is not subject to copyright protection in the United States.

with 0.45 μm pores and diluted with RPMI culture medium. Seven serial dilutions were performed to reach concentrations of 100.0, 50.0, 25.0, 12.5, 6.25, 3.125, 1.56, and 0.78% of extract. The pure medium was used as a negative control.

In a 96-well plate, 2×10^4 cells per well were seeded with RPMI supplemented with 1% glutamine, 1% antibiotic, and 1% fetal bovine serum (w/v). The plates were then incubated for 24 h. Subsequently, the culture medium was removed, and the extracts were added according to their respective dilutions. The plates were incubated again for another 24 h. Then, the extracts were removed, the wells were washed 2 times with PBS, and the neutral red solution was added. After 3 h of incubation, the medium was removed and an acid-ethanolic solution [1% glacial acetic acid, 50% ethanol, and 49% distilled water (v/v)] was added to each plate, which were shaken for 10 min. Finally, the optical density (OD) of each well was measured by an ELISA reader at a wavelength of 540 nm. The cell viability was calculated as follows:

$$\text{Cell viability}(\%) = \left(\text{OD}_{\text{Sample}}/\text{OD}_{\text{Control}}\right) \times 100\% \quad .$$

Zone of inhibition test

The antimicrobial activity test on KGM membranes was assessed using the modified agar diffusion method according to Ponce et al. [27]. The zone of inhibition assay on solid media was used for determining the antimicrobial effects of membranes against four typical pathogens—*Escherichia coli* (ATCC 8739), *Pseudomonas aeruginosa* (ATCC 9027), *Staphylococcus aureus* (ATCC 6538), and *Candida albicans* (ATCC 10231). The membranes samples were cut into discs of 10 mm of diameter, decontaminated with 70% (v/v) ethanol for 2 h, and then rinsed with PBS. Next, the samples were placed on agar plates, which had been previously seeded with 5 mL of inoculums containing approximately 10^6 CFU/mL of the tested microorganisms. The plates were then incubated at 37 °C for 24 h for the bacterial strains and at 25 °C for 48 h for the yeast strain. After the incubation period, the diameter of the inhibitory zone surrounding the sample discs as well as the contact area was measured.

Microbial penetration test

The membrane's ability to prevent microbial penetration was tested based on the methodology developed by Wittaya-areekul and Prahsarn [28]. Ionizing radiation–sterilized polyvinyl chloride (PVC) fittings were embedded in glass vials containing 50 mL of TSB medium (trypticase soy broth). Then, the membrane samples (diameter of 5 cm) were placed between the PVC fittings and the glass vials. All samples were decontaminated with ethanol 70% (v/v) or 2 h and then rinsed with PBS. The negative control was a sealed system with PVC film. The positive control was an open vial. All systems were incubated for 10 days under room conditions. Any cloudiness on the TBS medium was assigned as contamination by microorganisms.

Acknowledgments

Genevro was supported through the fellowship 13/18958-6 granted by São Paulo Research Foundation (FAPESP). The authors also thank the Brazilian National Council of Technological and Scientific Development (CNPq) for the financial support.

References

1. **P.I. Morgado, A. Aguiar-Ricardo, and I.J. Correia**: Asymmetric membranes as ideal wound dressings: An overview on production methods, structure, properties, and performance relationship. *J. Membr. Sci.* **490**, 139 (2015).
2. **A.J. Whittam, Z.N. Maan, D. Duscher, V.W. Wong, J.A. Barrera, M. Januszyk, and G.C. Gurtner**: Challenges and opportunities in drug delivery for wound healing. *Adv. Wound Care* **5**, 79 (2016).
3. **J. Koehler, F.P. Brandl, and A.M. Goepferich**: Hydrogel wound dressings for bioactive treatment of acute and chronic wounds. *Eur. Polym. J.* **100**, 1 (2018).
4. **L. Pachuau**: Recent developments in novel drug delivery systems for wound healing. *Expet Opin. Drug Deliv.* **12**, 1895 (2015).
5. **J.S. Boateng, K.H. Matthews, H.N.E. Stevens, and G.M. Eccleston**: Wound healing dressings and drug delivery systems: A review. *J. Pharm. Sci.* **97**, 2892 (2008).
6. **R. Xu, H. Xia, W. He, Z. Li, J. Zhao, B. Liu, Y. Wang, Q. Lei, Y. Kong, Y. Bai, Z. Yao, R. Yan, H. Li, R. Zhan, S. Yang, G. Luo, and J. Wu**: Controlled water vapor transmission rate promotes wound-healing via wound re-epithelialization and contraction enhancement. *Sci. Rep.* **6**, 24596 (2016).
7. **W.L.J. Hinrichs, E. Lommen, C.R.H. Wildevuur, and J. Feijen**: Fabrication and characterization of an asymmetric polyurethane membrane for use as a wound dressing. *J. Appl. Biomater.* **3**, 287 (1992).
8. **Y. Chen, L. Yan, T. Yuan, Q. Zhang, and H. Fan**: Asymmetric polyurethane membrane with in situ-generated nano-TiO_2 as wound dressing. *J. Appl. Polym. Sci.* **119**, 1532 (2011).
9. **F.L. Mi, Y.B. Wu, S.S. Shyu, J.Y. Schoung, Y.B. Huang, Y.H. Tsai, and J.Y. Hao**: Control of wound infections using a bilayer chitosan wound dressing with sustainable antibiotic delivery. *J. Biomed. Mater. Res.* **59**, 438 (2002).
10. **F.L. Mi, Y.B. Wu, S.S. Shyu, A.C. Chao, J.Y. Lai, and C.C. Su**: Asymmetric chitosan membranes prepared by dry/wet phase separation: A new type of wound dressing for controlled antibacterial release. *J. Membr. Sci.* **212**, 237 (2003).
11. **P.I. Morgado, P.F. Lisboa, M.P. Ribeiro, S.P. Migue, P.C. Simoes, I.J. Correia, and A. Aguiar-Ricardo**: Poly(vinyl

https://doi.org/10.1557/jmr.2018.463 Published online by Cambridge University Press

© Materials Research Society 2019. This is a work of the U.S. Government and is not subject to copyright protection in the United States.

alcohol)/chitosan asymmetrical membranes: Highly controlled morphology toward the ideal wound dressing. *J. Membr. Sci.* **469**, 262 (2014).

12. **C. Tang, Y. Guan, S. Yao, and Z. Zhu**: Preparation of drug-loaded asymmetric chitosan films towards wound dressing using supercritical solution impregnation. *Acta Polym. Sin.* **6**, 774 (2014).
13. **H. Xu, J. Chang, Y. Chen, H. Fan, and B. Shi**: Asymmetric polyurethane membrane with inflammation-responsive antibacterial activity for potential wound dressing application. *J. Mater. Sci.* **48**, 6625 (2013).
14. **Y. Xie, Z-X. Yi, J-X. Wang, T-G. Hou, and Q. Jiang**: Carboxymethyl konjac glucomannan—Crosslinked chitosan sponges for wound dressing. *Int. J. Biol. Macromol.* **112**, 1225–1233 (2018).
15. **H.N. Mamani Chambi and C.R. Ferreira Grosso**: Mechanical and water vapor permeability properties of biodegradables films based on methylcellulose, glucomannan, pectin and gelatin. *Cienc. Tecnol. Aliment.* **31**, 739 (2011).
16. **M. Shahbuddin, S. MacNeil, and S. Rimmer**: Synthesis and preparation of konjac glucomannan hydrogel for wound healing. *J. Tissue Eng. Regener. Med.* **6**, 1 (2012).
17. **Y-C. Huang, H-W. Chu, C-C. Huang, W-C. Wu, and J-S. Tsai**: Alkali-treated konjac glucomannan film as a novel wound dressing. *Carbohydr. Polym.* **117**, 778 (2015).
18. **X. Du, L. Yang, X. Ye, and B. Li**: Antibacterial activity of konjac glucomannan/chitosan blend films and their irradiation-modified counterparts. *Carbohydr. Polym.* **92**, 1302 (2013).
19. **X. Ni, F. Ke, M. Xiao, K. Wu, Y. Kuang, H. Corke, and F. Jiang**: The control of ice crystal growth and effect on porous structure of konjac glucomannan-based aerogels. *Int. J. Biol. Macromol.* **92**, 1130 (2016).
20. **X. Luo, P. He, and X. Lin**: The mechanism of sodium hydroxide solution promoting the gelation of Konjac glucomannan (KGM). *Food Hydrocolloids* **30**, 92 (2013).
21. **Z. Li, Y. Su, B. Xie, X. Liu, X. Gao, and D. Wang**: A novel biocompatible double network hydrogel consisting of konjac glucomannan with high mechanical strength and ability to be freely shaped. *J. Mater. Chem. B* **3**, 1769 (2015).
22. **ASTM: D882-02, Standard Test Method for Tensile Properties of Thin Plastic Sheeting (1995).**
23. **B. S. EN:** 13726-1:2002, Test methods for primary wound dressings: *Moisture Vapor Transmission Rate Permeable Film Dressings* (2002).
24. **S. Thomas and S. Young**: Exudate-handling mechanisms of two foam-film dressings. *J. Wound Care* **17**, 309 (2008).
25. **T.L. Riss, R.A. Moravec, A.L. Niles, S. Duellman, H.A. Benink, T.J. Worzella, and L. Minor:** In eds., G.S. Sittampalam, N.P. Coussens, K. Brimacombe, A. Grossman, M. Arkin, D. Auld, C. Austin, J. Baell, B. Bejcek, J.M.M. Caaveiro, T.D.Y. Chung, J.L. Dahlin, V. Devanaryan, T.L. Foley, M. Glicksman, M.D. Hall, J.V. Haas, J. Inglese, P.W. Iversen, S.D. Kahl, S.C. Kales, M. Lal-Nag, Z. Li, J. McGee, O. McManus, T. Riss, O.J.O.J. Trask, J.R. Weidner, M.J. Wildey, M. Xia, and X. Xu (Bethesda, MD, 2004).
26. **I.S.O. 10993-5 (2009).**
27. **A.G. Ponce, R. Fritz, C. del Valle, and S.I. Roura**: Antimicrobial activity of essential oils on the native microflora of organic Swiss chard. *LWT - Food Sci. Technol.* **36**, 679 (2003).
28. **S. Wittaya-areekul and C. Prahsarn**: Development and in vitro evaluation of chitosan-polysaccharides composite wound dressings. *Int. J. Pharm.* **313**, 123 (2006).
29. **S.J. Hollister**: Porous scaffold design for tissue engineering (vol 4, pg 518, 2005). *Nat. Mater.* **5**, 590 (2006).
30. **N-Y. Yuan, Y-A. Lin, M-H. Ho, D-M. Wang, J-Y. Lai, and H-J. Hsieh**: Effects of the cooling mode on the structure and strength of porous scaffolds made of chitosan, alginate, and carboxymethyl cellulose by the freeze-gelation method. *Carbohydr. Polym.* **78**, 349 (2009).
31. **M. Kita, Y. Ogura, Y. Honda, S.H. Hyon, W.I. Cha, and Y. Ikada**: Evaluation of polyvinyl-alcohol hydrogel as a soft contact-lens material. *Graefe's Arch. Clin. Exp. Ophthalmol.* **228**, 533 (1990).
32. **R. Ma and D. Xiong**: Synthesis and properties of physically crosslinked poly(vinyl alcohol) hydrogels. *J. China Univ. Min. Technol.* **18**, 4 (2008).
33. **H. Yu, Y. Huang, H. Ying, and C. Xiao**: Preparation and characterization of a quaternary ammonium derivative of konjac glucomannan. *Carbohydr. Polym.* **69**, 29 (2007).
34. **L. Liu, D. Hu, G. Xu, L. Shou, and J. Yao**: Fabrication and evaluation of polyurethane-based asymmetric membranes. *J. Mater. Sci.* **48**, 1902 (2013).
35. **J.J. Elsner and M. Zilberman**: Novel antibiotic-eluting wound dressings: An in vitro study and engineering aspects in the dressing's design. *J. Tissue Viability* **19**, 54 (2010).
36. **K. Wang and Z.M. He**: Alginate-konjac glucomannan-chitosan beads as controlled release matrix. *Int. J. Pharm.* **244**, 117 (2002).
37. **F.H. Silver, J.W. Freeman, and D. DeVore**: Viscoelastic properties of human skin and processed dermis. *Skin Res. Technol.* **7**, 18 (2001).
38. **A. Ní Annaidh, K. Bruyère, M. Destrade, M.D. Gilchrist, and M. Otténio**: Characterization of the anisotropic mechanical properties of excised human skin. *J. Mech. Behav. Biomed. Mater.* **5**, 139 (2012).
39. **B. Hansen and G.B. Jemec**: The mechanical properties of skin in osteogenesis imperfecta. *Arch. Dermatol.* **138**, 909 (2002).
40. **S. Banker Gilbert**: Film coating theory and practice. *J. Pharm. Sci.* **55**, 81 (1966).
41. **I.V. Yannas, J.F. Burke, M. Warpehoski, P. Stasikelis, E.M. Skrabut, D.P. Orgill, and D. Giard**: *Biomaterials: Interfacial Phenomena and Applications* (American Chemical Society, Washington DC, 1982); pp. 475–481.
42. **L. Ruiz-Cardona, Y.D. Sanzgiri, L.M. Benedetti, V.J. Stella, and E.M. Topp**: Application of benzyl hyaluronate membranes as

https://doi.org/10.1557/jmr.2018.463 Published online by Cambridge University Press

© Materials Research Society 2019. This is a work of the U.S. Government and is not subject to copyright protection in the United States.

potential wound dressings: Evaluation of water vapour and gas permeabilities. *Biomaterials* **17**, 1639 (1996).

43. **L.O. Lamke, G.E. Nilsson, and H.L. Reithner**: The evaporative water loss from burns and the water-vapour permeability of grafts and artificial membranes used in the treatment of burns. *Burns* **3**, 159 (1977).
44. **W. Zhu, J. Li, J. Lei, Y. Li, T. Chen, T. Duan, W. Yao, J. Zhou, Y. Yu, and Y. Liu**: Silver nanoparticles incorporated konjac glucomannan-montmorillonite nacre-like composite films for antibacterial applications. *Carbohydr. Polym.* **197**, 253 (2018).
45. **J. Lu, X. Wang, and C. Xiao**: Preparation and characterization of konjac glucomannan/poly(diallydimethylammonium chloride) antibacterial blend films. *Carbohydr. Polym.* **73**, 427 (2008).
46. **D.M.P. Spolidorio and C. Duque**: *Microbiologia e Imunologia Geral e Odontológica: Série Abeno: Odontologia Essencial—Parte Básica*, Vol. **2** (Artes Médicas Editora, Sao Paulo, Brazil, 2013).

https://doi.org/10.1557/jmr.2018.463 Published online by Cambridge University Press

© Materials Research Society 2019. This is a work of the U.S. Government and is not subject to copyright protection in the United States.